Published in final edited form as:
Pain. 2011 December ; 152(12): 2746–2756. doi:10.1016/j.pain.2011.08.022.

Functional Brain Activation during Retrieval of Visceral Pain-Conditioned Passive Avoidance in the Rat

Zhuo Wang[1,7], **Sylvie Bradesi**[1,3], **Jonathan R. Charles**[4], **Raina D. Pang**[5], **Jean-Michel I. Maarek**[6], **Emeran A. Mayer**[1,2,3], and **Daniel P. Holschneider**[1,3,5,6,7,8]

[1]Center for the Neurobiology of Stress, Dept. of Medicine, University of California, Los Angeles, CA

[2]Dept. of Physiology, Psychiatry & Biobehavioral Sciences, Brain Research Institute, University of California, Los Angeles, CA

[3]VA GLA Healthcare System, Los Angeles, CA

[4]Dept. of Chemistry & Biochemistry, California State University, Los Angeles, CA

[5]Program in Neuroscience; University of Southern California, Los Angeles, CA.

[6]Dept. of Biomedical Engineering, University of Southern California, Los Angeles, CA.

[7]Dept. of Psychiatry and the Behavioral Sciences, University of Southern California, Los Angeles, CA.

[8]Depts. of Cell & Neurobiology, Neurology, University of Southern California, Los Angeles, CA.

INTRODUCTION

Symptom related anxiety and maladaptive coping (e.g., “catastrophizing”, worst case assumption of pain outcomes) play a prominent role in the pathophysiology of persistent pain disorders, including irritable bowel syndrome (IBS) [8,28,67]. Importantly, expectation of pain established through associative learning can lead to affective responses similar to that evoked by acute pain, as well as coping responses that modulate subsequent pain perception. It has been hypothesized that while the effective coping responses in healthy people involve activation of a cortico-limbic-pontine inhibitory network that inhibits pain perception, failure of this inhibitory mechanism may contribute to hyperalgesia in persistent pain disorders [5,35,56,62,71].

In light of the critical involvement of erroneous outcome predictions in chronic pain disorders, an increasing number of human brain imaging studies have focused on understanding the neural substrates of pain expectation. Many of the general brain regions activated during acute pain are also activated in expectation of pain [11,21,40,49,51,72], including the anterior insula (aINS), dorsolateral prefrontal cortex (dorsolateral PFC), and anterior midcingulate cortex (MCC).

Corresponding author: Daniel P. Holschneider, MD, University of Southern California, 1333 San Pablo St., BMT 403, MC9112, Los Angeles, CA 90033, Tel: (323)442-1536, Fax: (323)442-1587, holschne@usc.edu.

There are no conflicts of interest.

In contrast to the rapidly growing human brain imaging research on pain expectation, there has been limited animal research in this field. Lei et al. [31] studied brain c-fos expression in rats during recall of formalin-conditioned place avoidance, and showed that similar brain regions expressed c-fos as those during acute formalin treatment. Our group have previously applied an autoradiographic blood flow mapping method to the colorectal distension (CRD) model of visceral pain [68,69]. Acute CRD induced activation in the aINS, anterior cingulate cortex (ACC), PFC (prelimbic area, PrL), and amygdala, in close agreement with human findings. Such functional brain mapping in rodent models of pain can serve as a translational tool to bridge preclinical and clinical pain research [19]. To map functional brain activation in expectation of visceral pain, we applied blood flow mapping to the step-down passive avoidance (PA) model using CRD as the aversive conditioning stimulus.

Passive avoidance (inhibitory avoidance) is a well-studied model of aversive learning, having both Pavlovian and operant components (reviewed in [32,37,61]). Converging evidence has implicated the basolateral amygdala and dorsal hippocampus in the acquisition, consolidation, and expression of PA. The step-down version of PA has been successfully applied to validate the aversive nature of several distension-based visceral pain models [42,44,45,57]. Whereas animal research has focused mostly on the learning and memory aspect of PA, not enough attention has been given to the affective component associated with expectation of aversive stimuli. We hypothesize that during the retrieval phase of PA, in addition to regions implicated in PA expression, brain regions implicated in the processing of the affective component of visceral pain also show increased activation. The study provides further validation for using the functional brain mapping method to delineate central mechanisms underlying the affective responses associated with pain expectation. Such platform can be used to validate animal models of functional pain disorders at the brain level, and to assess drug responses in these models.

METHODS

Animals

Twenty-two adult, male Wistar rats were randomized into two groups: conditioned and control (n = 11 / group). Rats were received from the vendor (Harlan Sprague Dawley, Indianapolis, IN, USA) one week prior to experimentation and were individually housed in the vivarium on a 12 hr light/12 hr dark cycle with free access to water and rodent chow. All experiments were conducted under a protocol approved by the Institutional Animal Care and Use Committee of the University of Southern California and are in accordance with the guidelines of the Committee for Research and Ethical Issues of the International Association for the Study of Pain (IASP).

Surgical procedures

Animals were anesthetized (isoflurane 2 % in 70 % oxygen, 30 % nitrous oxide). The right external jugular vein was cannulated with a 5 French silastic catheter advanced into the superior vena cava. A port at the distal end of the catheter was tunneled subcutaneously and externalized dorsally in the region rostral to the scapula. Animals were allowed to recover for six days before training started. The catheter was flushed every other day postoperatively to ensure patency (0.3 mL of 0.9% saline, followed by 0.1 mL of saline with 20 U/mL heparin).

Step-down passive avoidance training

Figure 1 shows the experimental setup and timeline. Animals were habituated to a training arena (wall height = 40 cm, diameter = 60 cm) for 15 min the day before training (Day 0). Over the next two days (Day 1 and Day 2), animals were trained for 18 trials / day. Each

animal was instrumented with a colorectal balloon. Briefly, under light isoflurane anesthesia (1.5 % isoflurane × 2 min.), a flexible latex balloon (length: 6 cm) was inserted intra-anally such that its end was 1 cm proximal to the anus. The balloon was connected to a barostat (Distender Series II, G & J Electronics Inc., Toronto, Canada) through a piece of Tygon tubing (R-3603, Saint-Gobain Performance Plastics, Akron, OH, USA), which was fixed to the base of the tail with adhesive tape and covered by a stainless steel spring for protection against animal biting. The animal was allowed to recover for 30 min in a transit cage, the floor of which was covered with bedding from the animal's home cage. At the beginning of each training trial, the rat was put on an elevated platform (W × L × H: 13 × 13 × 10 cm) placed next to the wall in the training arena. Step-down latencies were recorded using a stopwatch to the nearest second as the time taken for the animal to step down by putting both forepaws on the arena floor. Upon stepping down, a conditioned rat received a 60-mmHg, 20-s CRD delivered through the barostat, whereas the balloon of a control rat remained un-inflated. Animals were then returned to the transit cage. If the animal remained on the platform for 120 s (cut-off time), it was returned to the transit cage, and step-down latency was recorded as 120 s. Each trial lasted 3 min, including the time spent in the transit cage. The protocol has been adapted from studies using step-down PA to validate animal models of visceral pain [42,44,45,57]. Whereas in previous studies, retrieval was assessed within the same training session, we modified the protocol so that we could assess functional brain activation during PA retrieval one day after training and in the absence of a balloon. The objective was to avoid possible confounding factors such as short-term stress associated with balloon insertion and CRD, and sensitization to the inserted balloon in the conditioned rats. The modifications included placing the platform next to the arena wall during training and recall, rather than in the center of the arena, and increasing the training trials to 18 per day for two days. The final protocol reflected a balanced approach to achieving a robust behavioral endpoint, while limiting the intensity of training to avoid excessive stress.

Retrieval of passive avoidance and cerebral perfusion

On Day 3, PA behavior was tested in the absence of a colorectal balloon. A piece of silastic tubing was filled with radiotracer [^{14}C]-iodoantipyrine (125 μCi/kg in 300 μL of 0.9% saline, American Radiolabelled Chemicals, St. Louis, MO, USA). The radiotracer-filled tubing was then connected to the animal's cannula on one end, and to a syringe filled with euthanasia agent (pentobarbital 75 mg/mL, 3 M potassium chloride) on the other. The animal was allowed to rest for 15 min in the transit cage before the retrieval trials. On the first trial, the animal was placed on the platform to record the step-down latency. The animal was put back into the transit cage immediately after stepping down, or after 120 s if it remained on the platform. On the second trial, 45 s after the animal was put on the platform, radiotracer was infused at 2.25 mL/min by a motorized pump, followed immediately by euthanasia, which resulted in cardiac arrest within ~ 10 s, a precipitous fall of arterial blood pressure, termination of brain perfusion, and death. This 10-s time window provided the temporal resolution for rCBF mapping.

Brain slicing and autoradiography

Brains were rapidly removed, flash frozen in dry ice/methylbutane (~ -55 °C) and embedded in OCT compound (Sakura Fintek Inc., Torrance, CA, USA). Brains were subsequently sectioned on a cryostat (HM550 Series, Microm International GmbH, Walldorf, Germany) at -20 °C into 20-μm-thick coronal slices, with an inter-slice sampling space of 300 μm. Slices were heat-dried on glass slides and exposed for 2 weeks at room temperature to Ektascan Diagnostic Film (Eastman Kodak Co., Rochester, NY, USA). Images of brain sections were then digitized using an 8-bit gray scale.

Functional brain mapping data analysis

rCBF-related tissue radioactivity was quantified by autoradiography and analyzed on a whole-brain basis using SPM (version SPM5, Wellcome Centre for Neuroimaging, University College London, London, UK). Recently, we and others have developed and validated an adaptation of SPM for use in rodent brain autoradiograph [12,20,30,43]. In preparation for the SPM analysis, a 3-dimensional reconstruction of each animal's brain was conducted using 57 serial coronal sections (starting at ~ bregma + 4.5 mm) with a voxel size of 40 μm × 300 μm × 40 μm. Adjacent sections were aligned both manually and using TurboReg, an automated pixel-based registration algorithm implemented in ImageJ (http://rsbweb.nih.gov/ij/). This algorithm registered each section sequentially to the previous section using a nonwarping geometric model that included rotations and translations (rigid-body transformation) and nearest-neighbor interpolation. Global mean of voxel optical density was computed for each brain, and proportional scaling was performed to normalize optical density across brains. One “artifact free” brain was selected as reference. All brains were spatially normalized to the reference brain. Spatial normalization consisted of applying a 12-parameter affine transformation followed by a nonlinear spatial normalization using 3D discrete cosine transforms. All normalized brains were averaged to create the final rat brain template. Each original 3D-reconstructed brain was then spatially normalized to the template. Normalized brains were smoothed with a Gaussian kernel (FWHM = 3 × voxel dimension in the coronal plane). A nonbiased, voxel-by-voxel analysis of regional brain activation was performed in SPM. Voxels for each brain failing to reach a specified threshold (70% of the mean voxel value) were masked out to eliminate the background and ventricular spaces without masking gray or white matter. We implemented a Student's *t*-test at each voxel, testing the null hypothesis that there was no effect of conditioning. Threshold for significance was set at $P < 0.05$ at the voxel level and an extent threshold of 100 contiguous voxels. This combination reflected a balanced approach to control both Type I and Type II errors. The minimum cluster criterion was applied to avoid basing our results on significance at a single or small number of suprathreshold voxels. Brain regions were identified according to a rat brain atlas [47].

Functional connectivity analysis

To understand organization of the underlying brain network, we performed functional connectivity analysis. Interregional correlation-based functional connectivity analysis has been applied on rodent brain imaging data to understand brain network activity underlying the resting state [46,55,73] and extinction of conditioned fear [4] among other behaviors [reviewed in 6]. More recently, graph theoretical analysis has been adapted to the study of functional and structural brain networks [reviewed in 7]. This method is particularly useful for visualizing overall network structure and identifying network hubs. We applied these methods to understand how brain regions interact at the network level during retrieval of visceral pain-conditioned PA.

We performed functional connectivity analysis based on inter-regional correlation of rCBF. Region of interest (ROI) was functionally defined as a set of voxels of a brain area showing significant increases in rCBF in conditioned, as compared to control rats. Anatomical ROIs were first drawn manually in MRIcro (version 1.40, http://cnl.web.arizona.edu/mricro.htm) over the template brain according to the rat brain atlas. A functional ROI was created by combining the anatomical ROI with the SPM clusters (contrast: conditioned – control, $P < 0.05$, extent threshold > 100 contiguous voxels) by logical conjunction. Mean optical density of each ROI was calculated for each animal using the Marsbar toolbox for SPM (version 0.42, http://marsbar.sourceforge.net/).

An inter-regional correlation matrix was calculated across animals for each group in Matlab (version 6.5.1, The MathWorks, Inc., Natick, MA, USA). The matrices were visualized as heatmaps with Pearson's correlation coefficients color-coded. Statistical significance of between-group difference of a correlation coefficient was evaluated using the Fisher's Z-transform test ($P < 0.05$) [15].

Graph theoretical analysis was performed on networks defined by the above correlation matrices in the Pajek software (version 2.03, http://vlado.fmf.uni-lj.si/pub/networks/Pajek/) [9]. Each ROI was represented by a vertex (node) in a graph, and two vertices with significant correlation (positive or negative) were linked with an edge. A Kamada-Kawai algorithm [24] was implemented to arrange the graph such that strongly connected regions were placed closer to each other, while weakly connected regions were placed further apart. Absolute values of correlation coefficients were used for the strength of connection.

To identify hubs of the networks, we calculated four centrality metrics in Pajek: betweenness, degree, closeness, and *k*-core [9,18]. Edges were converted to binary format for centrality calculation. The betweenness centrality of a vertex is defined as the fraction of shortest paths connecting any pair of other vertices that go through this vertex. Betweenness evaluates the importance of a vertex in connecting different parts of a network. A vertex with high betweenness is thus crucial to efficient communication. The degree of a vertex is defined as the number of edges linking it to the rest of the network. Intuitively, vertices with higher degrees are more extensively connected and more central in the network organization. The closeness centrality of a vertex is defined as the reciprocal of the average distance from the vertex to all the other vertices and is computed as the number of other vertices divided by the sum of shortest paths from this vertex to all others. Vertices with higher closeness can reach other parts of the network faster through the paths and are considered more central to the network. A *k*-core is a measure of modularity and indicates a maximal subnetwork in which every vertex has a degree greater or equal to *k*. It identifies clusters of vertices that are tightly connected to each other. To derive *k*-core of a graph, vertices with degree lower than *k* are recursively removed until none remain. Each vertex is assigned a *k*-core number, defined as the highest *k*-core that contains the vertex. Vertices ranked in the top 25^{th} percentile (top 8 of 30 ROIs) in a centrality measurement were considered hubs in the network.

Statistical analysis of step-down latency

A mixed model ANOVA was used to assess statistical significance between control and conditioned rats in Day 1 and Day 2 training. Student's *t*-test and Wilcoxon rank test were used for statistical comparison of the first and second retrieval trials on Day 3, respectively. The nonparametric Wilcoxon rank test was used because distribution of step-down latencies for the second trial was not normal due to the 45-s cut off time. $P < 0.05$ was considered statistically significant.

RESULTS

Conditioned rats acquired passive avoidance behavior

Figure 2 shows the step-down latency of rats during passive avoidance training (Day 1 and Day 2) and retrieval (Day 3). Over the two-day training, conditioned rats learned to stay on the platform to avoid the 60-mmHg CRD, showing greater step-down latencies than controls (Day 1, $F(1,20) = 1.6$, $P = 0.22$; Day 2, $F(1,20) = 6.8$, $P = 0.017$, mixed model ANOVA). The learned PA behavior was retrieved on Day 3 in the absence of the colorectal balloon. Conditioned rats showed significantly greater step-down latencies on the first trial (37 ± 6 s in conditioned rats vs. 15 ± 4 s in controls, $P = 0.01$, Student's *t*-test), as well as on the

second trial (36 ± 4 s in conditioned rats vs. 21 ± 5 s in controls, $P = 0.03$, Wilcoxon rank test). The presence of a balloon during training combined with repeated exposure to the platform may have caused habituation. This may account for the increase in step-down latency in the control rats during training, as well as the drop in step-down latency in both groups on Day 3 (without the balloon) as compared to trial 1, Day 2 (with the balloon). Step-down latency on Day 3 was likely a more accurate measurement of contextual recall of PA, without the nonspecific effect of an inserted balloon.

Functional brain activation during the retrieval of passive avoidance

Brain areas showing significant differences in rCBF between the conditioned and the control group are depicted in Figure 3 and summarized in Table 1. Compared to controls, conditioned animals showed increased rCBF bilaterally in a wide range of areas including medial PFC subregions (ventral cingulate, Cg2; right dorsal cingulate, Cg1; retrosplenial, RS, equivalent to posterior cingulate in primates; PrL), aINS, nucleus accumbens (NAcc), amygdala (including basolateral amygdala, BLA; amygdalopiriform transition area, APir; cortical amygdaloid nuclei, PLCo, PMCo), and dorsomedial periaqueductal gray(DMPAG). In addition, increased rCBF was noted bilaterally in primary motor cortex (M1), primary and secondary somatosensory cortices (S1, S2), as well as the anterior dorsal caudate putamen (adCPu), lateral caudate putamen (lCPu), dorsal hippocampus (dHPC), lateral septum (LS), and the cerebellum (vermis, CbVermis; hemisphere, CbHemis). White matter tracts, including the forceps minor of the corpus callosum (fmi) and external capsule (ec) bilaterally, and left anterior commissure (AC) also showed increased rCBF in conditioned rats. Significant decreases in rCBF were noted in the conditioned rats in the inferior colliculus (IC) and pontine nuclei (Pn) bilaterally, and in the entorhinal cortex (Ent) in the right hemisphere.

Shaded cells in Table 1 depict regions that also showed changes in rCBF in response to acute CRD as we previously reported [68]. Regions showing activation in both studies included the Cg1, PrL, aINS, S1, S2, M1, and adCPu, with differences noted in the extent of activation in these regions. Important differences in regional brain activation were also noted between these studies. In response to acute CRD, but not retrieval of CRD-conditioned PA, broader cortical areas, including the auditory and visual areas, as well as the central and lateral nuclei of the amygdala showed activation. In contrast, the BLA, dHPC, NAcc, DMPAG, and cerebellum showed activation only in the current study.

Functional connectivity of brain networks in the control rats

An inter-regional correlation matrix of rCBF was constructed for the control group and visualized as a heatmap in Figure 4A. Significant correlations ($P < 0.05$) were interpreted as functional connections and marked with white dots. The matrix is symmetric across the diagonal line from upper left to lower right, which itself reflects the trivial correlation of ROIs to themselves. There were 47 significant positive correlations and 15 significant negative correlations. A cluster of midline cortical ROIs, including bilateral Cg2, RS, PrL/PFC, and right Cg1, were strongly and positively correlated with each other. Within this cortical cluster, all except PrL/PFC were significantly positively correlated with striatal ROIs (including bilateral NAcc and adCPu), but negatively correlated with the amygdala. Intra-structural positive correlations were noted within the striatum, and the cerebellum. In addition, PrL/PFC, Cg2, RS, S1, NAcc, adCPu, dHPC, amygdala and the cerebellar hemispheres showed strong, positive cross-hemisphere correlations.

Graph theoretical analysis revealed organization of the functional network and hubs (Figure 4B, Table 2). The cortical cluster (Figure 4B, red vertices) is clearly shown in the center of the network, with its negative connections (dashed lines) to the amygdala and the

cerebellum (Figure 4B, blue vertices). ROIs in the above-mentioned cortical cluster (Cg2, right Cg1, RS, PrL) were identified as hubs together with bilateral adCPu. In addition, CbHemis, dHPC, and LS were identified as hubs by their high betweenness centrality.

Functional connectivity of brain networks in the conditioned rats

Figure 4C shows the inter-regional correlation matrix for the conditioned group. There were fewer connections in the conditioned group than in the controls, 25 positive and 16 negative significant correlations. Certain similarities in the functional connectivity pattern between the two groups were noted, including the intra-structural positive correlations in the cortex and the striatum, as well as positive correlations between the cortex and striatum, and negative correlations between the cortex and amygdala. Meanwhile, there were important group differences (Figure 5). In the cortex, M1 and PrL/PFC showed more connectivity with other cortical areas, whereas RS showed less connectivity in the conditioned group. Strong positive connections were seen between the amygdala and cerebellar hemispheres. The amygdala was negatively connected to PrL/PFC in the conditioned group, whereas in the controls the amygdala was negatively connected to RS. In addition, M1, S1, PrL/PFC, Cg2, RS, aINS, adCPu, dHPC, amygdala and the cerebellar hemisphere showed positive cross-hemisphere correlation.

Graph analysis revealed a cortical cluster, with RS seemingly removed from the core (Figure 4D, red vertices). The amygdala and cerebellum in conditioned animals formed a separate cluster, and were negatively connected to the cortical cluster (PrL/PFC, Cg1, Cg2). The NAcc, PrL/PFC, and aINS were shown to be crucial to the network structure, with the highest betweenness centrality. In addition, cingulate cortex (Cg1, Cg2), adCPu, and amygdala were also identified as network hubs by graph analysis (Table 2).

DISCUSSION

Our main findings were: (1) During the retrieval of visceral pain-conditioned PA, conditioned rats showed activation in the prelimbic area of the prefrontal, anterior insular, and anterior cingulate cortices - areas previously shown to be activated during acute noxious visceral stimulation [17,68]; (2) Conditioned rats also showed activation in the basolateral amygdala, dorsal hippocampus, and nucleus accumbens - regions implicated in memory recall of PA; (3) In the control group, connectivity analysis revealed a corticostriatal core, which connected negatively to the amygdala, mainly through the retrosplenial cortex. (4) In the conditioned group, by contrast, a modified corticostriatal core connected negatively to the amygdala through the prelimbic area of the medial prefrontal cortex, which, together with the nucleus accumbens and anterior insula, emerged as network hubs. Whereas the brain circuits underlying PA memory recall and affective responses associated with expected pain are likely intertwined, and the current protocol does not dissociate these circuits, we discuss our findings in two separate sections to reflect our interpretation of the data based on the literature.

Expectation of visceral pain: Comparison to human brain imaging literature

The findings of similar activation of key brain regions during expected pain as during acute noxious CRD [68], are in agreement with human brain imaging findings implicating homologous regions (aINS, anterior MCC, dorsolateral PFC) in central processing of actual and expected visceral pain [5,41,72]. The insula, the primary interoceptive cortex, is the most commonly reported brain region activated by acute visceral noxious stimulation in humans [34,60]. Based on a meta-analysis of human imaging studies, it was concluded that the anterior basal insula shows dense connections to the amygdala and limbic areas, whereas the anterior dorsal insula is more closely associated with frontal association areas [27]. This

pattern of functional connectivity in humans correlates with reported anatomical connectivity in the monkey [2]. Using a classical conditioning paradigm, Yaguez et al. showed activation of anterior insula during expectation of esophageal distension in healthy subjects [72]. In contrast, Berman et al. showed in healthy subjects reduced activation of the anterior insula during a cued anticipatory period preceding rectal distension [5]. The observation of bi-directional modulation of anterior insula suggests different anticipatory and coping responses.

Subregions of the cingulate cortex have frequently been implicated in the affective and motivational response to pain [35,65], including the rostral ACC and anterior MCC. Homology in cingulate regions between primate and rodent is an evolving subject [66]. Cg1 area in the rat is considered homologous to ACC and dorsal aspects of MCC in primates, while Cg2 area in the rat is homologous to ventral aspects of MCC in primates, and RS in the rat is homologous to posterior cingulate cortex (PCC) in primates. In humans, the anterior MCC is activated during acute visceral pain, and slightly more rostral aspects of anterior MCC in expectation of visceral pain [54,72]. This is consistent with the activation of Cg1 during acute CRD [68] and activation of Cg1 and Cg2 in the conditioned rats in the current study. Cingulate lesions in animals cause severe deficits in avoidance behavior to noxious somatic stimuli [23,26]. Interestingly, Gao et al. [16] reported that lesion to the Cg1 region selectively impairs formalin-induced, but not footshock-induced, place avoidance learning, suggesting that this region specifically mediates pain-related negative affect.

We noted an almost identical activation of the PrL/PFC in conditioned rats and in rats receiving acute CRD [68]. The exact homology between rodents and primates in regions of the PFC remains unresolved [63]. The PrL in the rat is generally considered part of medial PFC, with features of dorsolateral PFC [63,64] and ACC [52,66]. Activation of dorsolateral PFC, ventrolateral PFC, and medial PFC in response to visceral pain have been reported in humans [reviewed by 34], and activation of these regions has been implicated in corticolimbic inhibition [33,48,70]

Functional brain activation associated with the expression of passive avoidance

Passive avoidance is an extensively studied model of aversive learning. A majority of studies have used electric footshock as the aversive stimulus in either a step-down or a step-through design. Of particular relevance to our study, key brain regions critically involved in the retrieval of PA have been reported to include the basolateral amygdala, dorsal hippocampus, and striatum, including the nucleus accumbens [32]. Our results provide the first blood flow mapping evidence implicating all these regions in PA retrieval. Functional activation of the basolateral amygdala is consistent with the notion that this structure plays a critical role in the encoding and storage of emotional memory [14]. Increases in rCBF were also noted in the nearby amygdalopiriform transition area, the function of which is not well understood, but which has been proposed to play a role in the expression of emotional and motivated behaviors [53]. The dorsal hippocampus is believed to process contextual information required for the retrieval, consistent with its well-established role in contextual Pavlovian fear conditioning and spatial memory tasks [13]. The nucleus accumbens may play a role in evaluating aversive cues and mediating behavioral responses [10], whereas dorsal striatum mediates important aspects of decision-making [3,10].

Conditioned rats also showed robust activation in the cerebellum. The cerebellum plays a critical role in classical conditioning and motor learning [59], as well as in mediating autonomic nervous system responses [74]. Steinmetz et al. [58] showed that bilateral lesions of deep cerebellar nuclei impair the learning of an aversive bar pressing task, but not an appetitive task, suggesting a critical role in aversive operant learning. Activation of the cerebellum has been noted in anticipation of somatic [25,49,50], as well as visceral pain [72]

in humans, although the functional implication is not well understood. Moulton et al. [39] proposed recently that the cerebellum may act as an integrator of multiple effectors systems, including sensorimotor processing, affective processing, pain modulation, and autonomic responses.

Network analysis

Correlational and graph theoretical analysis revealed a number of findings not immediately apparent from the regional analysis in SPM. In control rats, a corticostriatal core was revealed that demonstrated strong positive correlations between midline cortical regions, including Cg1/ACC, Cg2/anterior MCC, PrL/PFC, RS/PCC, as well as with NAcc and adCPu. Within this corticostriatal core, Cg2 and RS were negatively correlated with the amygdala, while the PrL/PFC was negatively correlated with the cerebellum. In an analysis of interregional correlation of cerebral metabolic rates in the awake 'resting state' in rats, Soncrant et al. [55] also reported positive correlations between PFC, frontal cortex, NAcc, and striatum. Andrews-Hanna et al. reported in human subjects a midline core (consisting of PCC and anterior medial PFC) for the human brain "default network", a functional network consistently observed in human functional imaging studies when subjects are in a resting state [1]. While the function of the default network is still not well understood, our results suggest that some features of the network may be preserved across species.

In conditioned animals, the correlation patterns were similar, though less extensive, than those noted in controls. Uniquely, conditioned rats showed 1) a loss of significant correlation between the RS/PCC and the amygdala, as well as between the RS/PCC and the striatum (NAcc, adCPu); 2) a negative correlation between the amygdala and PrL/PFC; 3) positive correlations between the amygdala and cerebellar hemispheres; and 4) a significant positive cross-hemisphere correlation in aINS, and a positive correlation between aINS and NAcc.

Graph theoretical analysis underscored these findings. In conditioned animals, the PrL/PFC emerged as a clear hub, which connected both locally (as a provincial hub) and to other modules (as a connector hub). Locally, the PrL/PFC served as a hub within the corticostriatal core. The RS/PCC was notably dissociated from this core, in contrast to its inclusion in the core in the control animals. The 'PFC-centric' cluster was negatively correlated to the amygdala, which functioned as a connector hub to a smaller module comprised of itself and the cerebellar hemispheres. The negative connection between the PFC and amygdala is consistent with the notion of reciprocal inhibitory modulation between these regions in emotion and pain processing [22,36,38]. Of note, recent work by Labus et al. examining brain responses to aversive visceral stimuli in IBS patients showed that rostral ACC exerts a significant negative influence on the amygdala in male subjects during expectation of visceral pain [29]. In addition, our data revealed that the 'PFC-centric' cluster connected via the NAcc (a connector hub) to a smaller module comprised of the NAcc, aINS, motor and somatosensory areas.

In conclusion, we established an animal model to study brain mechanisms underlying the affective responses associated with visceral pain expectation. Important specificity issues remain to be addressed since brain circuits underlying pain processing of different modalities as well as other emotional processing often overlap significantly. Reverse translation from human brain imaging findings may help interpretation of animal imaging data. Homologous findings at the circuit level between the rodent and human functional brain imaging suggests that neuroimaging may provide a means for bidirectional translation between preclinical and clinical pain research, with implications for the future identification of novel therapeutic targets in the modulatory network of visceral pain processing.

Acknowledgments

Grant support from GlaxoSmithKline, and the Animal Models Core and the Neuroimaging Core of the Center for Neurobiology of Stress, UCLA (NIDDK P50DK064539, NCCAM AT00268) is acknowledged.

REFERENCES

1. Andrews-Hanna JR, Reidler JS, Sepulcre J, Poulin R, Buckner RL. Functional-anatomic fractionation of the brain's default network. Neuron. 2010; 65:550–562. [PubMed: 20188659]
2. Augustine JR. Circuitry and functional aspects of the insular lobe in primates including humans. Brain Res Brain Res Rev. 1996; 22:229–244. [PubMed: 8957561]
3. Balleine BW, Delgado MR, Hikosaka O. The role of the dorsal striatum in reward and decision-making. J Neurosci. 2007; 27:8161–8165. [PubMed: 17670959]
4. Barrett D, Shumake J, Jones D, Gonzalez-Lima F. Metabolic mapping of mouse brain activity after extinction of a conditioned emotional response. J Neurosci. 2003; 23:5740–5749. [PubMed: 12843278]
5. Berman SM, Naliboff BD, Suyenobu B, Labus JS, Stains J, Ohning G, Kilpatrick L, Bueller JA, Ruby K, Jarcho J, Mayer EA. Reduced brainstem inhibition during anticipated pelvic visceral pain correlates with enhanced brain response to the visceral stimulus in women with irritable bowel syndrome. J Neurosci. 2008; 28:349–359. [PubMed: 18184777]
6. Bifone A, Gozzi A, Schwarz AJ. Functional connectivity in the rat brain: a complex network approach. Magn Reson Imaging. 2010; 28:1200–1209. [PubMed: 20813478]
7. Bullmore E, Sporns O. Complex brain networks: graph theoretical analysis of structural and functional systems. Nat Rev Neurosci. 2009; 10:186–198. [PubMed: 19190637]
8. Crombez G, Vlaeyen JW, Heuts PH, Lysens R. Pain-related fear is more disabling than pain itself: evidence on the role of pain-related fear in chronic back pain disability. Pain. 1999; 80:329–339. [PubMed: 10204746]
9. de Nooy, W.; Mrvar, A.; Batagelj, V. Exploratory social network analysis with Pajek. Cambridge University Press; Cambridge: 2005.
10. Delgado MR, Li J, Schiller D, Phelps EA. The role of the striatum in aversive learning and aversive prediction errors. Philos Trans R Soc Lond B Biol Sci. 2008; 363:3787–3800. [PubMed: 18829426]
11. Drevets WC, Burton H, Videen TO, Snyder AZ, Simpson JR Jr. Raichle ME. Blood flow changes in human somatosensory cortex during anticipated stimulation. Nature. 1995; 373:249–252. [PubMed: 7816140]
12. Dubois A, Herard AS, Flandin G, Duchesnay E, Besret L, Frouin V, Hantraye P, Bonvento G, Delzescaux T. Quantitative validation of voxel-wise statistical analyses of autoradiographic rat brain volumes: application to unilateral visual stimulation. Neuroimage. 2008; 40:482–494. [PubMed: 18234520]
13. Fanselow MS, Dong HW. Are the dorsal and ventral hippocampus functionally distinct structures? Neuron. 2010; 65:7–19. [PubMed: 20152109]
14. Fanselow MS, LeDoux JE. Why we think plasticity underlying Pavlovian fear conditioning occurs in the basolateral amygdala. Neuron. 1999; 23:229–232. [PubMed: 10399930]
15. Fisher RA. On the ‘probable error’ of a coefficient of correlation deduced from a small sample. Metron. 1921; 1:3–32.
16. Gao YJ, Ren WH, Zhang YQ, Zhao ZQ. Contributions of the anterior cingulate cortex and amygdala to pain- and fear-conditioned place avoidance in rats. Pain. 2004; 110:343–353. [PubMed: 15275785]
17. Gibney SM, Gosselin RD, Dinan TG, Cryan JF. Colorectal distension-induced prefrontal cortex activation in the Wistar-Kyoto rat: implications for irritable bowel syndrome. Neuroscience. 2010; 165:675–683. [PubMed: 19765638]
18. Hagmann P, Cammoun L, Gigandet X, Meuli R, Honey CJ, Wedeen VJ, Sporns O. Mapping the structural core of human cerebral cortex. PLoS Biol. 2008; 6:e159. [PubMed: 18597554]

19. Holschneider DP, Bradesi S, Mayer EA. The role of experimental models in developing new treatments for irritable bowel syndrome. Expert Rev Gastroenterol Hepatol. 2011; 5:43–57. [PubMed: 21309671]
20. Holschneider DP, Yang J, Sadler TR, Nguyen PT, Givrad TK, Maarek JM. Mapping cerebral blood flow changes during auditory-cued conditioned fear in the nontethered, nonrestrained rat. Neuroimage. 2006; 29:1344–1358. [PubMed: 16216535]
21. Hsieh JC, Stone-Elander S, Ingvar M. Anticipatory coping of pain expressed in the human anterior cingulate cortex: a positron emission tomography study. Neurosci Lett. 1999; 262:61–64. [PubMed: 10076873]
22. Ji G, Sun H, Fu Y, Li Z, Pais-Vieira M, Galhardo V, Neugebauer V. Cognitive impairment in pain through amygdala-driven prefrontal cortical deactivation. J Neurosci. 2010; 30:5451–5464. [PubMed: 20392966]
23. Johansen JP, Fields HL, Manning BH. The affective component of pain in rodents: direct evidence for a contribution of the anterior cingulate cortex. Proc Natl Acad Sci U S A. 2001; 98:8077–8082. [PubMed: 11416168]
24. Kamada T, Kawai S. An algorithm for drawing general undirected graphs. Information Processing Letters. 1988; 31:7–15.
25. Keltner JR, Furst A, Fan C, Redfern R, Inglis B, Fields HL. Isolating the modulatory effect of expectation on pain transmission: a functional magnetic resonance imaging study. J Neurosci. 2006; 26:4437–4443. [PubMed: 16624963]
26. Kung JC, Su NM, Fan RJ, Chai SC, Shyu BC. Contribution of the anterior cingulate cortex to laser-pain conditioning in rats. Brain Res. 2003; 970:58–72. [PubMed: 12706248]
27. Kurth F, Zilles K, Fox P, Laird A, Eickhoff S. A link between the systems: functional differentiation and integration within the human insula revealed by meta-analysis. Brain Structure and Function. 2010; 214:519. [PubMed: 20512376]
28. Labus JS, Mayer EA, Chang L, Bolus R, Naliboff BD. The central role of gastrointestinal-specific anxiety in irritable bowel syndrome: further validation of the visceral sensitivity index. Psychosom Med. 2007; 69:89–98. [PubMed: 17244851]
29. Labus JS, Naliboff BN, Fallon J, Berman SM, Suyenobu B, Bueller JA, Mandelkern M, Mayer EA. Sex differences in brain activity during aversive visceral stimulation and its expectation in patients with chronic abdominal pain: A network analysis. Neuroimage. 2008; 41:1032–1043. [PubMed: 18450481]
30. Lee JS, Ahn SH, Lee DS, Oh SH, Kim CS, Jeong JM, Park KS, Chung JK, Lee MC. Voxel-based statistical analysis of cerebral glucose metabolism in the rat cortical deafness model by 3D reconstruction of brain from autoradiographic images. Eur J Nucl Med Mol Imaging. 2005; 32:696–701. [PubMed: 15747156]
31. Lei LG, Zhang YQ, Zhao ZQ. Pain-related aversion and Fos expression in the central nervous system in rats. Neuroreport. 2004; 15:67–71. [PubMed: 15106833]
32. Liang KC. Involvement of the Amygdala and Its Connected Structures in Formation and Expression of Inhibitory Avoidance Memory: Issues and Implications. Chinese Journal Of Physiology. 2009; 52:196–214.
33. Lorenz J, Minoshima S, Casey KL. Keeping pain out of mind: the role of the dorsolateral prefrontal cortex in pain modulation. Brain. 2003; 126:1079–1091. [PubMed: 12690048]
34. Mayer EA, Aziz Q, Coen S, Kern M, Labus JS, Lane R, Kuo B, Naliboff B, Tracey I. Brain imaging approaches to the study of functional GI disorders: a Rome working team report. Neurogastroenterol Motil. 2009; 21:579–596. [PubMed: 19646070]
35. Mayer EA, Naliboff BD, Craig AD. Neuroimaging of the brain-gut axis: from basic understanding to treatment of functional GI disorders. Gastroenterology. 2006; 131:1925–1942. [PubMed: 17188960]
36. Mayer J, Schuster HG, Claussen JC. Role of inhibitory feedback for information processing in thalamocortical circuits. Phys Rev E Stat Nonlin Soft Matter Phys. 2006; 73:031908. [PubMed: 16605559]
37. McGaugh JL. The amygdala modulates the consolidation of memories of emotionally arousing experiences. Annu Rev Neurosci. 2004; 27:1–28. [PubMed: 15217324]

38. Moont R, Crispel Y, Lev R, Pud D, Yarnitsky D. Temporal changes in cortical activation during conditioned pain modulation (CPM), a LORETA study. Pain. 2011
39. Moulton EA, Schmahmann JD, Becerra L, Borsook D. The cerebellum and pain: passive integrator or active participator? Brain Res Rev. 2010; 65:14–27. [PubMed: 20553761]
40. Naliboff BD, Berman S, Suyenobu B, Labus JS, Chang L, Stains J, Mandelkern MA, Mayer EA. Longitudinal change in perceptual and brain activation response to visceral stimuli in irritable bowel syndrome patients. Gastroenterology. 2006; 131:352–365. [PubMed: 16890589]
41. Naliboff BD, Derbyshire SW, Munakata J, Berman S, Mandelkern M, Chang L, Mayer EA. Cerebral activation in patients with irritable bowel syndrome and control subjects during rectosigmoid stimulation. Psychosom Med. 2001; 63:365–375. [PubMed: 11382264]
42. Ness TJ, Randich A, Gebhart GF. Further behavioral evidence that colorectal distension is a 'noxious' visceral stimulus in rats. Neurosci Lett. 1991; 131:113–116. [PubMed: 1791969]
43. Nguyen PT, Holschneider DP, Maarek JM, Yang J, Mandelkern MA. Statistical parametric mapping applied to an autoradiographic study of cerebral activation during treadmill walking in rats. Neuroimage. 2004; 23:252–259. [PubMed: 15325372]
44. Nijsen MJ, Ongenae NG, Coulie B, Meulemans AL. Telemetric animal model to evaluate visceral pain in the freely moving rat. Pain. 2003; 105:115–123. [PubMed: 14499427]
45. Ozaki N, Bielefeldt K, Sengupta JN, Gebhart GF. Models of gastric hyperalgesia in the rat. Am J Physiol Gastrointest Liver Physiol. 2002; 283:G666–676. [PubMed: 12181181]
46. Pawela CP, Biswal BB, Cho YR, Kao DS, Li R, Jones SR, Schulte ML, Matloub HS, Hudetz AG, Hyde JS. Resting-state functional connectivity of the rat brain. Magn Reson Med. 2008; 59:1021–1029. [PubMed: 18429028]
47. Paxinos, G.; Watson, C. The rat brain in stereotatic coordinates. Elsevier Academic Press; New York: 2007.
48. Petrovic P, Kalso E, Petersson KM, Ingvar M. Placebo and opioid analgesia-- imaging a shared neuronal network. Science. 2002; 295:1737–1740. [PubMed: 11834781]
49. Ploghaus A, Tracey I, Gati JS, Clare S, Menon RS, Matthews PM, Rawlins JN. Dissociating pain from its anticipation in the human brain. Science. 1999; 284:1979–1981. [PubMed: 10373114]
50. Porro CA, Baraldi P, Pagnoni G, Serafini M, Facchin P, Maieron M, Nichelli P. Does anticipation of pain affect cortical nociceptive systems? J Neurosci. 2002; 22:3206–3214. [PubMed: 11943821]
51. Porro CA, Cettolo V, Francescato MP, Baraldi P. Functional activity mapping of the mesial hemispheric wall during anticipation of pain. Neuroimage. 2003; 19:1738–1747. [PubMed: 12948728]
52. Preuss TM. Do Rats Have Prefrontal Cortex - The Rose-Woolsey-Akert Program Reconsidered. Journal Of Cognitive Neuroscience. 1995; 7:1–24.
53. Shammah-Lagnado SJ, Santiago AC. Projections of the amygdalopiriform transition area (APir). A PHA-L study in the rat. Ann N Y Acad Sci. 1999; 877:655–660. [PubMed: 10415677]
54. Silverman DH, Munakata JA, Ennes H, Mandelkern MA, Hoh CK, Mayer EA. Regional cerebral activity in normal and pathological perception of visceral pain. Gastroenterology. 1997; 112:64–72. [PubMed: 8978344]
55. Soncrant TT, Horwitz B, Holloway HW, Rapoport SI. The pattern of functional coupling of brain regions in the awake rat. Brain Res. 1986; 369:1–11. [PubMed: 3697734]
56. Song GH, Venkatraman V, Ho KY, Chee MW, Yeoh KG, Wilder-Smith CH. Cortical effects of anticipation and endogenous modulation of visceral pain assessed by functional brain MRI in irritable bowel syndrome patients and healthy controls. Pain. 2006; 126:79–90. [PubMed: 16846694]
57. Stam R, van Laar TJ, Wiegant VM. Physiological and behavioural responses to duodenal pain in freely moving rats. Physiol Behav. 2004; 81:163–169. [PubMed: 15059696]
58. Steinmetz JE, Logue SF, Miller DP. Using signaled barpressing tasks to study the neural substrates of appetitive and aversive learning in rats: behavioral manipulations and cerebellar lesions. Behav Neurosci. 1993; 107:941–954. [PubMed: 8136069]
59. Thompson RF. In search of memory traces. Annu Rev Psychol. 2005; 56:1–23. [PubMed: 15709927]

60. Tillisch K, Mayer EA, Labus JS. Quantitative meta-analysis identifies brain regions activated during rectal distension in irritable bowel syndrome. Gastroenterology. 2010; 140:91–100. [PubMed: 20696168]
61. Tinsley MR, Quinn JJ, Fanselow MS. The role of muscarinic and nicotinic cholinergic neurotransmission in aversive conditioning: comparing pavlovian fear conditioning and inhibitory avoidance. Learn Mem. 2004; 11:35–42. [PubMed: 14747515]
62. Tracey I, Bushnell MC. How neuroimaging studies have challenged us to rethink: is chronic pain a disease? J Pain. 2009; 10:1113–1120. [PubMed: 19878862]
63. Uylings HB, Groenewegen HJ, Kolb B. Do rats have a prefrontal cortex? Behav Brain Res. 2003; 146:3–17. [PubMed: 14643455]
64. Vertes RP. Differential projections of the infralimbic and prelimbic cortex in the rat. Synapse. 2004; 51:32–58. [PubMed: 14579424]
65. Vogt BA. Pain and emotion interactions in subregions of the cingulate gyrus. Nat Rev Neurosci. 2005; 6:533–544. [PubMed: 15995724]
66. Vogt, BA.; Vogt, L.; Farber, NB. Cingulate cortex and disease models.. In: Paxinos, G., editor. The rat nervous system. Academic Press; San Diego: 2004. p. 705-727.
67. Waddell G, Newton M, Henderson I, Somerville D, Main CJ. A Fear-Avoidance Beliefs Questionnaire (FABQ) and the role of fear-avoidance beliefs in chronic low back pain and disability. Pain. 1993; 52:157–168. [PubMed: 8455963]
68. Wang Z, Bradesi S, Maarek JM, Lee K, Winchester WJ, Mayer EA, Holschneider DP. Regional brain activation in conscious, nonrestrained rats in response to noxious visceral stimulation. Pain. 2008; 138:233–243. [PubMed: 18538929]
69. Wang Z, Guo Y, Bradesi S, Labus JS, Maarek JM, Lee K, Winchester WJ, Mayer EA, Holschneider DP. Sex differences in functional brain activation during noxious visceral stimulation in rats. Pain. 2009; 145:120–128. [PubMed: 19560270]
70. Wiech K, Kalisch R, Weiskopf N, Pleger B, Stephan KE, Dolan RJ. Anterolateral prefrontal cortex mediates the analgesic effect of expected and perceived control over pain. J Neurosci. 2006; 26:11501–11509. [PubMed: 17079679]
71. Wilder-Smith CH, Schindler D, Lovblad K, Redmond SM, Nirkko A. Brain functional magnetic resonance imaging of rectal pain and activation of endogenous inhibitory mechanisms in irritable bowel syndrome patient subgroups and healthy controls. Gut. 2004; 53:1595–1601. [PubMed: 15479679]
72. Yaguez L, Coen S, Gregory LJ, Amaro E Jr. Altman C, Brammer MJ, Bullmore ET, Williams SC, Aziz Q. Brain response to visceral aversive conditioning: a functional magnetic resonance imaging study. Gastroenterology. 2005; 128:1819–1829. [PubMed: 15940617]
73. Zhang N, Rane P, Huang W, Liang Z, Kennedy D, Frazier JA, King J. Mapping resting-state brain networks in conscious animals. J Neurosci Methods. 2010; 189:186–196. [PubMed: 20382183]
74. Zhu JN, Yung WH, Kwok-Chong Chow B, Chan YS, Wang JJ. The cerebellar-hypothalamic circuits: potential pathways underlying cerebellar involvement in somatic-visceral integration. Brain Res Rev. 2006; 52:93–106. [PubMed: 16497381]

Summary
Expectation of visceral pain in rats recruits brain areas implicated in acute pain processing and passive avoidance, homologous to findings in humans during pain anticipation.

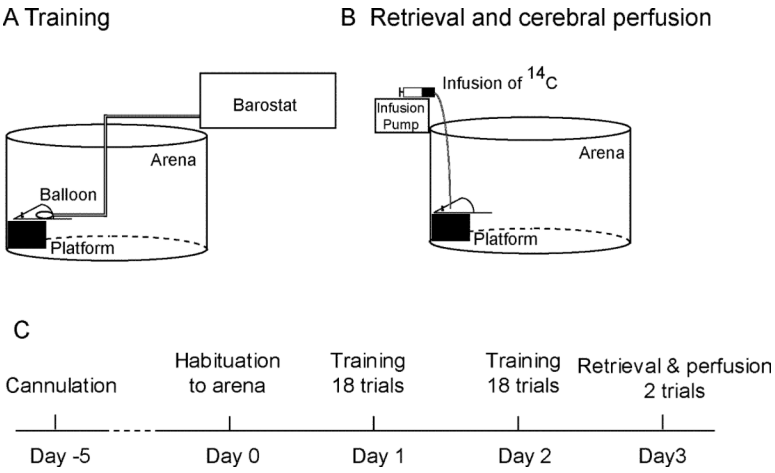

Figure 1.
Experimental setup and protocol

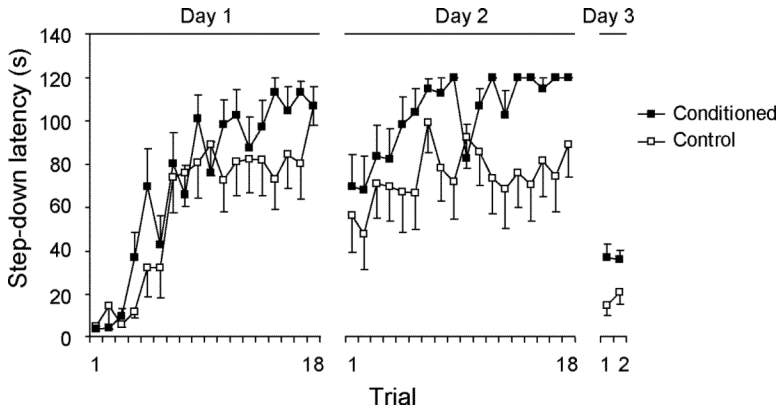

Figure 2. Acquisition and retrieval of step-down passive avoidance

After two days of training, the conditioned rats learned to refrain from stepping down to avoid the 60-mmHg, noxious colorectal distension (Day 1, $F(1,20) = 1.6$, $P = 0.22$; Day 2, $F(1,20) = 6.8$, $P = 0.017$, $n = 11$/group, mixed model ANOVA). This conditioned passive avoidance behavior was retrieved on Day 3 in the absence of the colorectal balloon. Step-down latencies were significantly greater in the conditioned group than in the controls on the first trial (37 ± 6 s vs. 15 ± 4 s, respectively, $P = 0.01$, Student's t-test), as well as on the second trial (36 ± 4 s vs. 21 ± 5 s, $P = 0.03$, Wilcoxon rank test). Standard error bars are depicted only unidirectionally for graphic clarity.

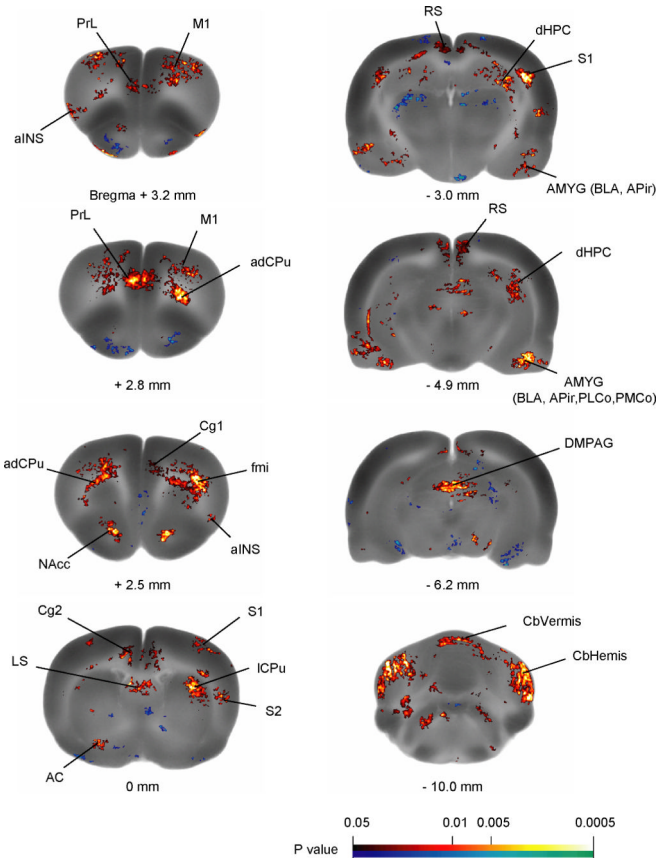

Figure 3. Key brain regions showing significant differences in regional cerebral blood flow between the conditioned and the control rats

Statistical parametric mapping (SPM) results contrasting the conditioned group to the control group show differences in regional cerebral blood flow during the retrieval of passive avoidance. Color-coded overlays show statistically significant positive (red) and negative (blue) changes in conditioned compared to control rats (n = 11/group, $P < 0.05$ at the voxel level with extend threshold of 100 contiguous voxels). Structural brain images are from the template brain at representative bregma levels. Abbreviations: aINS (anterior insular cortex); AC (anterior commissure); NAcc (n. accumbens); APir (amygdalopiriform transition area); BLA (basolateral amygdaloid n.); Cg1, Cg2 (cingulate cortex, area 1 and area 2); dHPC (dorsal hippocampus); DMPAG (dorsomedial periaqueductal gray); fmi (forceps minor of the corpus callosum); lCPu (lateral caudate putamen); LS (lateral septal n.); M1 (primary motor cortex); PMCo (posteromedial cortical amygdaloid n.); PLCo (posterolateral cortical amygdaloid n.); PrL (prelimbic cortex); RS (retrosplenial cortex); S1 (primary somatosensory cortex); S2 (secondary somatosensory cortex); Abbreviations are based on the Paxinos and Watson (2007) rat brain atlas with modifications for simplification.

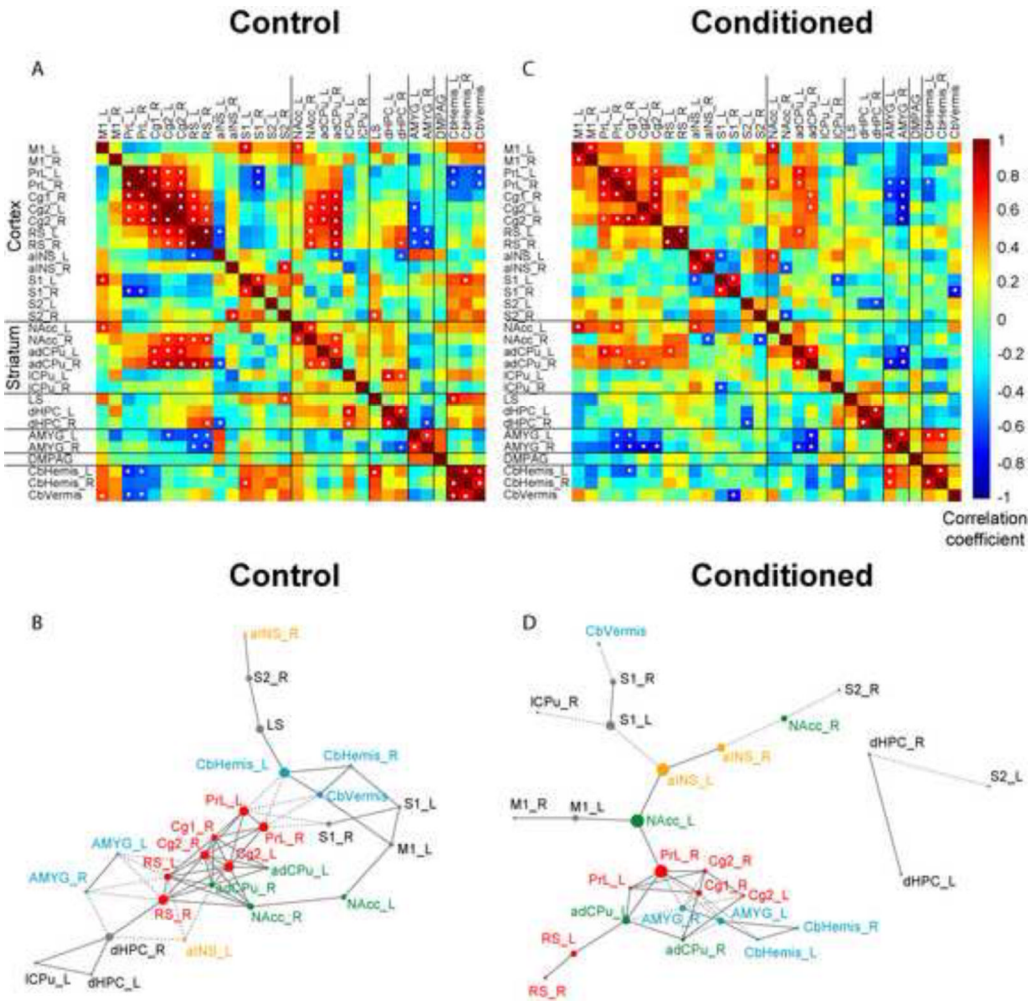

Figure 4. Functional connectivity analysis of network activation during retrieval of passive avoidance

Thirty regions of interest (ROIs) showing significant increases in regional cerebral blood flow in conditioned compared to control rats were entered into connectivity analysis. Abbreviations are as indicated in Figure 3 and Table 1. (A) Interregional correlation matrix for the control group. Pearson's correlation coefficients were color-coded. The matrix is symmetric across the diagonal line from upper left to lower right. Significant correlations ($P < 0.05$) were marked with white dots. Note the strong positive connections among cortical ROIs including PrL, Cg1, Cg2, RS, and striatal ROIs (NAcc, adCPu). Amygdala (AMYG) was negatively connected with this corticostriatal cluster. (B) Functional network for the control group is represented with a graph, in which vertices represent ROIs and edges represent significant correlations (connections). Solid lines denote positive correlations, whereas dashed lines negative correlations. The size of each vertex is proportional to its betweenness centrality, a measurement of how central a vertex is in a network. ROIs with the highest betweenness centrality were considered hubs of the network. Key vertices are color-coded to facilitate between-group comparison (unrelated to the color scale of A and C). (C) Interregional correlation matrix for the conditioned group. Note the reduced number of significant connections. AMYG was positively correlated with the cerebellum, and negatively correlated with PrL and Cg in the corticostriatal cluster. (D) Graph representation of the functional network in the conditioned group. NAcc, aINS, and AMYG were identified

as hubs of the network. ROIs in the right or left hemisphere are denoted with a suffix “R” or “L”, respectively.

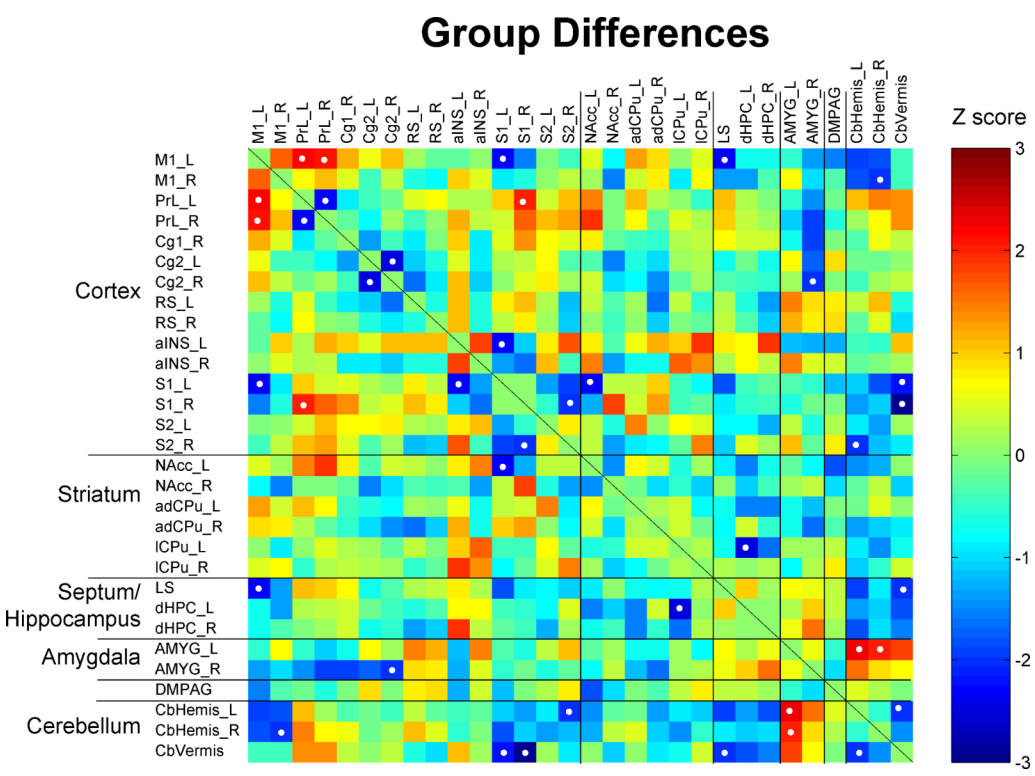

Figure 5. Changes in interregional correlation in the conditioned group compared to the controls

The matrix of Fisher's Z-statistics represents differences in Pearson's correlation coefficients (*r*) between the conditioned and control group. Positive Z values indicate increased *r* in the conditioned group, while negative Z values decreased *r*. Significant between-group differences ($P < 0.05$) were marked with white dots. Note the emergence of positive correlation between M1 and PrL, and between amygdala (AMYG) and cerebellar hemispheres (CbHemis). Also note trends of decreased correlations (less positive) in the cortical cluster (PrL, Cg1, Cg2, RS) and increased correlation (more negative) between the cortical cluster and the AMYG. ROIs in the right or left hemisphere are denoted with a suffix “R” or “L”, respectively. Abbreviations are as indicated in Figure 3 and Table 1.

Table 1

Brain regions showing significant changes in regional cerebral blood flow in conditioned rats compared to controls

Brain region	Left	Right
Cerebral cortex		
Cingulate, dorsal (Cg1, *homologous to human anterior cingulate and dorsal part of midcingulate, ACC, MCC, respectively)*		+
Cingulate, ventral (Cg2, *homologous to ventral part of human midcingulate, MCC*)	+	+
Insular, anterior (anteriorINS)	+	+
Motor, primary (M1)	+	+
Prelimbic (PrL, *homologous to part of human prefrontal cortex, PFC*)	+ *	+ *
Retrosplenial (RS, *homologous to human posterior cingulate, PCC*)	+	+
Somatosensory, primary (S1)	+	+ **
Somatosensory, secondary (S2)	+	+
Entorhinal (Ent)		- *
Subcortical regions		
Amygdala (AMYG), including basolateral (BLA) amygdalopiriform transition area (APir) cortical nuclei (PMCo, PLCo)	+	+ *
Caudate putamen, anterior dorsal (adCPu)	+	+
Caudate putamen, lateral (lCPu)	+ **	+ **
Cerebellum, hemisphere (CbHemis)	+ **	+ **
Cerebellum, vermis (CbVermis)	+ *	+ *
Corpus callosum, forceps minor (fmi)	+ *	+ *
External capsule (ec)	+ *	+ *
Hippocampus, dorsal (dHPC)	+	+ *
Lateral septal nucleus (LS)	+	+
Nucleus accumbens (NAcc)	+ *	+ *
Periaqueductal gray, dorsomedial (DMPAG)	+ *	+ *
Inferior colliculus (IC)	- *	-
Pontine nuclei (Pn)	-	-

Significant increases or decreases in regional blood flow are noted with '+' and '-', respectively, for the left and right hemispheres. Significance is shown at the voxel level ($P < 0.05$) with extent threshold of 100 contiguous voxels.

* Significant at the voxel level $P < 0.01$.

** Significant at the voxel level $P < 0.001$.

Shaded cells depict regions that showed changes in rCBF in response to acute colorectal distension (CRD) as we previously reported, with the difference that amygdalar activations during acute CRD were noted in the central and lateral nuclei, and changes in the lateral CPu and PAG showed a decrease rather than increase in rCBF [81].

Table 2

Hubs of the functional brain network

Control Rats

Rank	Betweenness	Degree	Closeness	k-core
1	CbHemis_L	Cg2_L	Cg2_L	adCPu R, NAcc R Cg2_L, Cg2_R RS_L, RS_R
2	RS_R	Cg2_R RS_L	Cg2_R	
3	Cg2_L		PrL_L	
4	PrL_L	adCPu_R RS_R	PrL_R	
5	PrL_R		Cg1_R	
6	dHPC_R	Cg1_R PrL_L PrL_R	RS_R	
7	LS		RS_L	adCPu_L, Cg1_R PrL_L, PrL_R
8	Cg2_R		NAcc_R	

Conditioned Rats

Rank	Betweenness	Degree	Closeness	k-core
1	NAcc_L	AMYG_R Cg1_R PrL_R	PrL_R	adCPu_L, adCPu_R AMYG_L, AMYG_R Cg1_R, Cg2_R PrL_L, PrL_R
2	PrL_R		NAcc_L	
3	aINS_L		aINS_L	
4	S1_L	AMYG_L	AMYG_R	
5	adCPu_L	adCPu_L adCPu_R Cg2_R	Cg1_R	
6	aINS_R		adCPu_L	
7	AMYG_L		AMYG_L	
8	M1_L	PrL_L	PrL_L	

Hubs of functional brain network were identified as region of interests (ROIs) ranked in the top 25 % in four measurements of centrality. Refer to Methods for detailed descriptions of the measurements. Abbreviations are as indicated in table 1. ROIs in the right or left hemisphere are denoted with suffixes “R” “L”, respectively.